International Journal of Advance Research in Science and Engineering
Vol. No.6, Issue No. 07, July 2017
www.ijarse.com
IJARSE
ISSN (O) 2319 - 8354
ISSN (P) 2319 - 8346

Photocatalytic Degradation of Rhodamine B dye using PPY/Ferricyanide Photoadduct Nanocomposite

Syed Kazim Moosvi[1], **Mohd. Abdullah Dar**[2]
Owais Mehraj[3], **Kowsar Majid**[4]
[1,2,3,4] *Department of Chemistry, National Institute of Technology*
Srinagar, J & K, (India)

ABSTRACT

Nanocomposite of polypyrrole (PPY) with ferricyanide photoadduct was synthesized via oxidative chemical polymerization method. The photoadduct of ferricyanide and triethylenetetramine (TETA) was synthesised by photoirradiation using Osram photolamp. The synthesis of photoadduct and PPY nanocomposite was confirmed by UV-Vis, FTIR, SEM and XRD characterization techniques. UV-Vis spectroscopic technique was used for studying the photocatalytic degradation of Rhodamine B dye in presence of synthesised nanocomposite. The synthesized nanocomposite exhibited a good photocatalytic activity for the degradation of Rhodamine B dye.

Keywords: Nanocomposite, Irradiation, Rhodamine B, PPY, Photocatalytic degradation kinetics.

I. INTRODUCTION

The discharge of coloured effluent from textile industries into water bodies like lakes, rivers and oceans results in severe environmental issues [1]. These coloured effluents are usually toxic and potentially carcinogenic hence considered as a menace to ecosystem [2]. These issues have caused public concern and responsiveness on water pollution. Although variety of physical, chemical and biological methods such as coagulation, adsorption, membrane process, and oxidation-ozonation have been employed for the treatment of dye wastewater , however, these methods do not lead to complete degradation of the dyes [3,4]. The heterogeneous photocatalytic process is a reliable technique, which can be successfully used to oxidize the organic pollutants present in the aqueous system [5, 6]. In this connection various organic/inorganic nanocomposites have been recently reported as promising photocatalytic materials for the degradation of harmful organic dye under light illumination [7]. Various photocatalytic materials such as ZnO–polyaniline, adsorbents as glass fibers, chitosan-g-poly(acrylic acid)/montmorillonite nanocomposite have been used for the remediation of harmful pollutants [8-11].

Among various conductive polymers, polypyrrole (PPY) is the most promising conductive polymer due to its good conductivity, electrochemical reversibility and the ease of preparation through chemical or electrochemical routes [12]. Nanocomposites of PPY with metal oxides have been well studied for photocatalytic activity [13, 14]. However, nanocomposites of PPY with transition metal complexes have not been investigated so much. In this direction our research group has investigated the photocatalytic activity of such type of nanocomposites which have been found to exhibit good photocatalytic activity [15, 16]. Keeping this in mind, we here report the synthesis of a nanocomposite of polypyrrole (PPY) with nanophotoadduct of potassium ferricyanide and triethylenetetramine (TETA) ligand. SEM, XRD and FTIR spectra were used here to investigate the morphology and structure of the products. The photocatalytic activity for the rhodamine B (RhB) dye degradation was investigated under light irradiation.

II. EXPERIMENTAL

2.1. Chemicals

Chemicals used in this work were pyrrole, potassium ferricyanide, anhydrous ferric chloride and triethylenetetramine (TETA) all supplied by Himedia, India. All the chemicals used were of analytical grade. Distilled deionised water was used throughout the experimental work.

2.2. Physical Measurements

UV-Vis absorption spectrum was recorded on double beam spectrophotometer (PG instruments T80). FTIR analysis was carried out by using Perkin Elmer RX–1, FTIR spectrophotometer. Irradiation was done with Osram UV photolamp. SEM analysis was done by using Hitachi SEM, Model S – 3600N. XRD pattern was obtained on PW 3050 base diffractometer, operating with Cu-Kα radiations ($\lambda = 1.54060$Å).

2.3. Synthesis of Nanophotoadduct

The photoadduct of $K_3[Fe(CN)_6]$ and triethylenetetramine (TETA) was synthesised by irradiating an equimolar mixture of $K_3[Fe(CN)_6]$ and TETA in water for some time using Osram photolamp till the color of the mixture changed from yellow to blackish. The product was then isolated through crystallization technique. The photoadduct was reduced to nanosize by ball milling using 15 zirconium balls of 5 mm size for 8 hrs at 450 rpm. The product obtained was then subjected to various spectroscopic and surface characterization techniques.

2.4. Synthesise of PPY/ nanophotoadduct Composite

The nanocomposite of PPY with synthesised photoadduct was achieved via oxidative chemical polymerisation method using $FeCl_3$ as oxidant. In a typical experiment, 0.055M $FeCl_3$ in 180 mL of chloroform was added drop wise to the stirred solution of 0.022M (in 70 mL chloroform) of distilled pyrrole monomer containing one gram of homogenised nanophotoadduct. The mixture was kept on stirring for 12 hours. After 12 hours, product was filtered and washed several times in order to remove impurities. The black powder was then dried at room temperature.

2.5 Photocatalytic activity

The photocatalytic activity of the nanocomposite was studied against Rhodamine B (RhB) dye in presence of UV-Vis light using Mercury-Xenon arc lamp. 0.1g of nanocomposite was suspended into the 50 ppm aqueous solution of RhB (100ml). Prior to irradiation the suspension was stirred for half an hour in dark. Then the suspension was irradiated under Mercury-Xenon arc lamp. At the given time intervals small aliquots of samples were collected from the suspension and analysed by a UV-Vis double beam spectrophotometer (PG instruments T80).

III. RESULTS AND DISCUSSIONS

3.1. UV -Visible characterization

The UV-Vis spectra of an aqueous solution mixture of $K_3[Fe(CN)_6]$ and TETA was recorded before and after irradiation. Before irradiation two peaks at 234 and 459 nm were observed in the absorption spectrum of the mixture (Fig.1(a)). Whereas, after irradiation the peak at 234 was red shifted to 242 nm (Fig. 1(b)). This change in absorption spectra of mixture before and after irradiation indicated the formation of photoadduct [17].

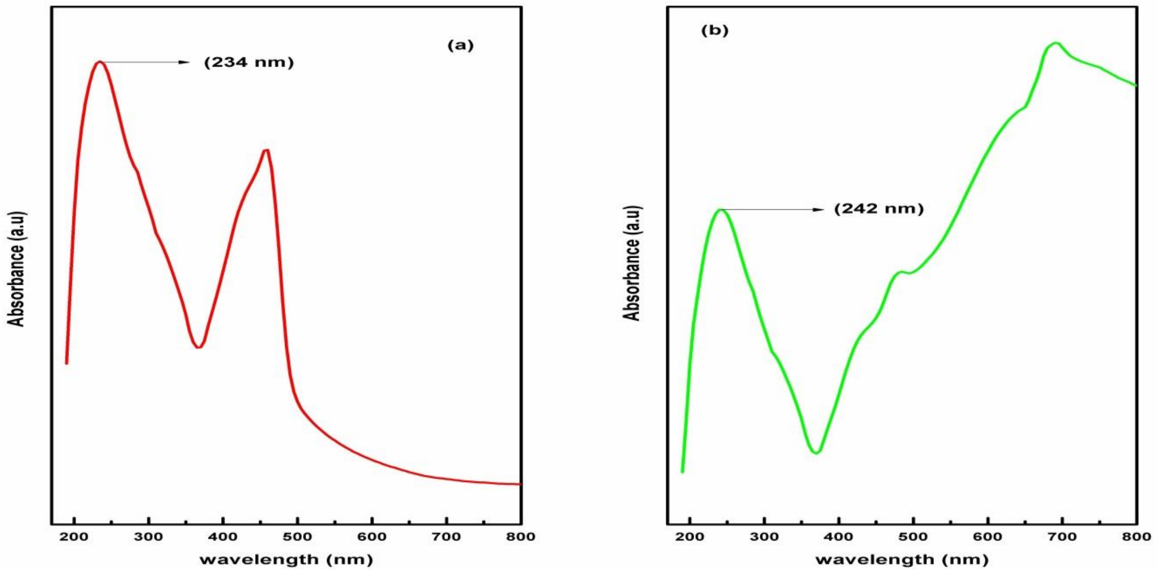

Fig.1: UV-Visible spectra of : aqueous solution of $K_3[Fe(CN)_6]$ and triethylenetetramine (TETA) (a) before irradiation and (b) after irradiation.

3.2. FTIR Characterization

FTIR spectra of nanophotoadduct and nanocomposite are shown in Fig.2 (a, b). The FTIR spectra of photoadduct as shown in Fig. 2 (a) shows characteristic peaks of both $K_3[Fe(CN)_6]$ and TETA though with some shifts, thus proving the successful formation of photoadduct [15]. FTIR spectra of PPY nanocomposite show the presence of a peak at 2095 cm^{-1} (Fig. 2(b)), which is due to ν (C≡N). This peak appears at 2045 cm^{-1} in the nanophotoadduct with a strong intensity. Thus a shifting of absorption peak by 50 cm^{-1} indicates the successful insertion of nanophotoadduct in the polypyrrole matrix. The insertion of photoadduct in PPY matrix is also evident by appearance of other absorption peaks of TETA in the polymer matrix.

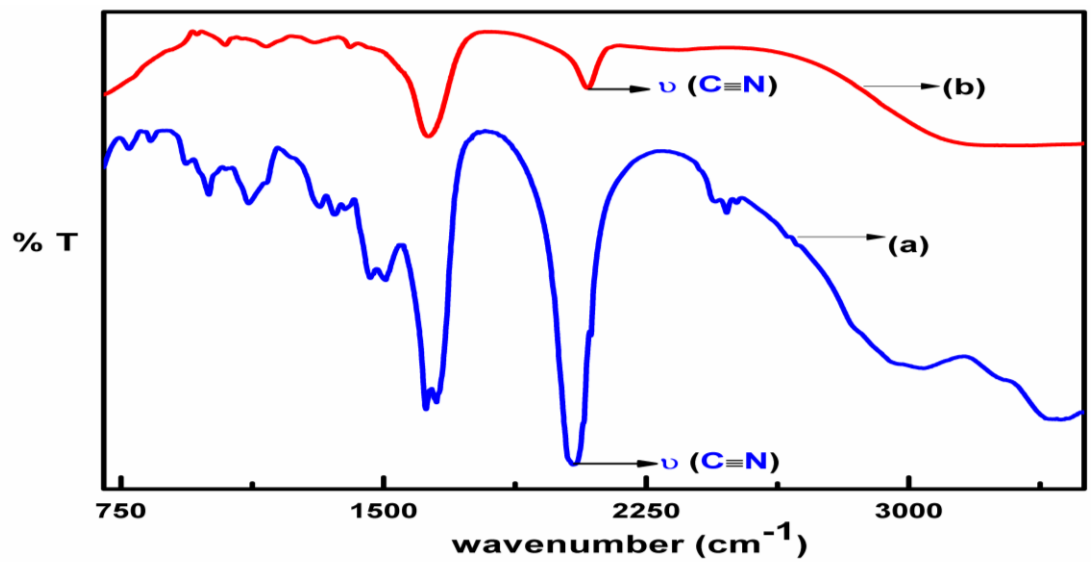

Fig.2: FTIR spectra of (a) nanophotoadduct, (b) nanocomposite.

3.3. XRD

The XRD diffraction pattern of nanophotoadduct and nanocomposite is presented in Fig.3 (a, b) respectively. PPY shows a hump at 2 theta value of 30° which indicates its amorphous nature [18]. The XRD pattern of nanophotoadduct shows presence of sharp peaks indicating its crystalline nature. The crystalline nature of photoadduct is retained in the nanocomposite. This again confirms the presence of nanophotoadduct in the polymer matrix. The average crystallite size of nanophotoadduct and nanocomposite was calculated using Scherrer formula and comes out to be 21 nm and 23 nm respectively.

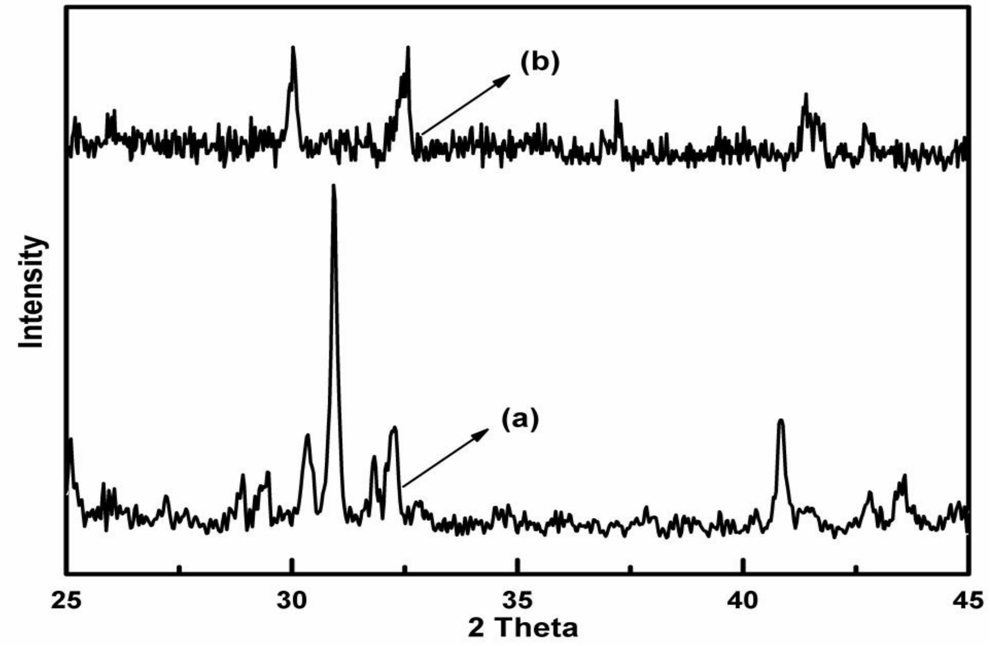

Fig 3: XRD of (a) nanophotoadduct, (b) nanocomposite.

3.4 SEM characterization

Fig. 4(a, b) shows the SEM micrographs of nanophotoadduct and PPY nanocomposite respectively. SEM micrograph of photoadduct shows agglomerated needle like crystals. SEM micrograph of pure PPY shows grooves and spongy nature [19]. However, the SEM micrograph of composite shows different surface morphology than pure photoadduct and PPY. This indicates the successful formation of composite.

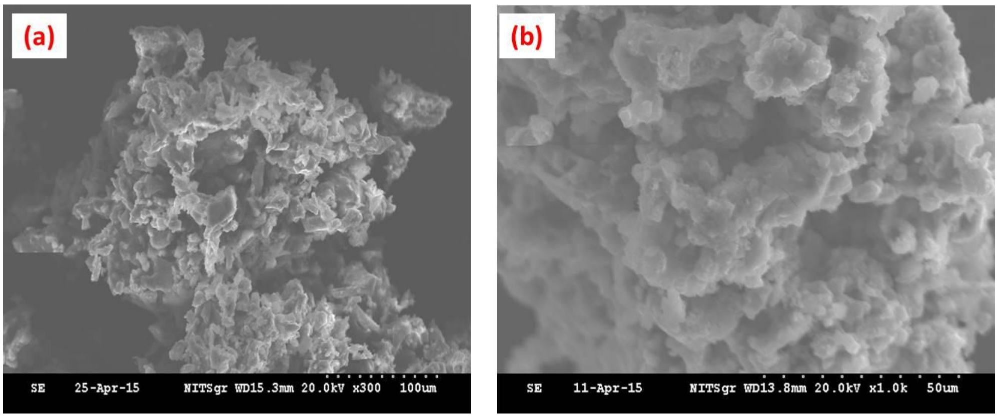

Fig.4: SEM micrographs of (a) nanophotoadduct, (b) nanocomposite.

3.5. Photocatalytic activity

The photode gradation experiment of nanocomposite was investigated against Rhodamine B dye in presence of UV-Visible light. The absorption spectrum of RhB dye with increasing illumination time is depicted in Figure 5 (a) which clearly shows the photodegradation of dye with time. The dye degradation plot of PPY nanocomposites is shown in Fig. 5 (b).

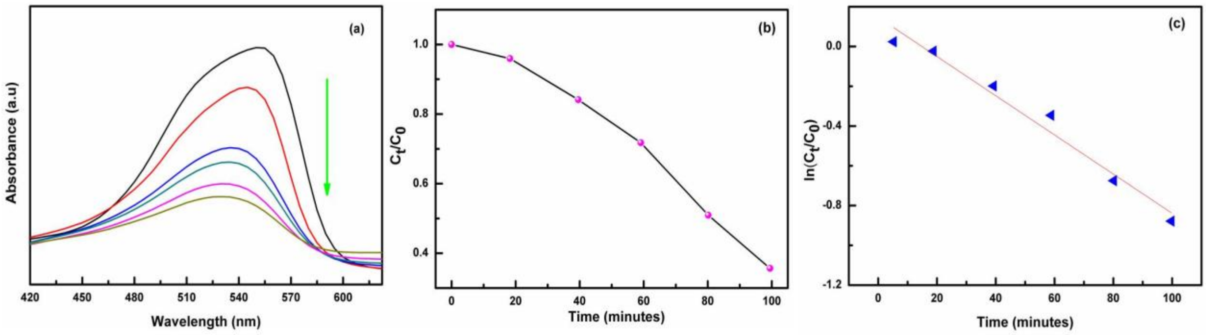

Fig.5: (a) Absorption spectra of RhB dye with increasing illumination time, (b) Plot of C_t/C_0 with time in presence of nanocomposite and (c) Linear fitting of the photocatalytic data. The percentage dye degradation was calculated using the formula:

% Degradation = $\frac{C_0-C_t}{C_0}\times 100$

where C_0 is the initial concentration of dye before illumination and C_t after time t.

73% degradation of RhB dye was achieved in 100 minutes. The photocatalytic activity begins with the generation of electron hole pairs in the catalyst under UV-Vis light [20]. These photoelectrons and holes react with the adsorbed O_2, OH^- and H_2O to form radical species like $O_2^{\bullet -}$, $^{\bullet}OH$, and $HO^{\bullet}_2$ etc. The radical species ($O_2^{\bullet -}$, $^{\bullet}OH$, and $HO^{\bullet}_2$) thus generated retort with the RhB dye to form degradation products [21].

Kinetics of the photodegradation rates of dye was also studied and was found to fit a pseudo first-order kinetic model that is $\ln(C_t/C_0) = -K_{obs}t$ where C_0 and C_t are the concentration of RhB dye at time 0 and t, respectively . The K_{obs} is the observed pseudo first-order rate constant and t is the time. The value of k_{obs} was found to be 9.8

$\times 10^{-3}$ min^{-1}. Thus nanocomposite can be applied as an effective photocatalyst for the degradation of organic dye pollutants.

IV. CONCLUSION

A nanocomposite of PPY and ferricyanide photoadduct was successfully synthesised which was confirmed from FTIR, XRD and SEM characterization techniques. The nanocomposite exhibited good photocatalytic activity against Rh B dye degradation.

V. ACKNOWLEDGEMENT

The authors are thankful to SAIF Chandigarh, SAIF STIC Kochi, and NIT Hamirpur for providing the instrumentation facilities.

REFERENCES

[1] J. Orfao J, A. Silva, J. Pereira, S. Barata, I. Fonseca and P. Faria, Adsorption of reactive dye on chemically modified activated carbons influence of pH. Journal of Colloid and Interface Science, 296, 2006, 480-489.

[2] M. Yazdanbakhsh, , I. Khosravi, , E.K. Goharshadi, and A..Youssefi, Fabrication of nanospinel $ZnCr_2O_4$ using sol–gel method and its application on removal of azo dye from aqueous solution. Journal of hazardous materials, 184, 2010, 684-689.

[3] A. Kumar, P. Chaudhary and P. Verma, Adsorption of reactive red 194 dye from textile effluent by using class F fly ash, Scholars journal of Applied Medical Sciences 1, 2013, 111-116.

[4] M.M. Alam, M.B. Mukhlish, S. Uddin, S. Das, K. Ferdous, M.R. Khan and M.A. Islam, Photocatalytic degradation of reactive yellow in batch and continuous photoreactor using titanium dioxide. Journal of Scientific Research, 4, 2012, 665-674.

[5] M.N. Abellán, B. Bayarri, J. Giménez, and J. Costa, Photocatalytic degradation of sulfametho xazole in aqueous suspension of TiO_2. Applied Catalysis B: Environmental, 74, 2007, 233-241.

[6] M.B. Mukhlish, F. Najnin, M.M. Rahman, and M.J. Uddin, Photocatalytic degradation of different dyes using TiO_2 with high surface area: a kinetic study. Journal of Scientific Research, 5, 2013, 301-314.

[7] S. Ameen, H.K. Seo, M.S. Akhtar, H.S. Shin, Novel graphene/polyaniline nanocomposites and its photocatalytic activity toward the degradation of rose Bengal dye. Chemical engineering journal, 210, 2012, 220-228.

[8] D. Pathania, G. Sharma, A. Kumar and N.C. Kothiyal, Fabrication of nanocomposite polyaniline zirconium (IV) silicophosphate for photocatalytic and antimicrobial activity. Journal of Alloys and Compounds, 588, 2014, 668-675.

[9] R. Gong, Y. Sun, J. Chen, H. Liu, and C. Yang, Effect of chemical modification on dye adsorption capacity of peanut hull. Dyes and pigments, 67, 2005, 175-181.

[10] N. Barka, A. Assabbane, A. Nounah, L. Laanab and Y.A. Ichou. Removal of textile dyes from aqueous solutions by natural phosphate as a new adsorbent. Desalination, 235, 2009, 264-275.

[11] L. Wang, J. Zhang and A. Wang. Removal of methylene blue from aqueous solution using chitosan-g-poly (acrylic acid)/montmorillonite super adsorbent nanocomposite. Colloids and Surfaces A: Physicochemical and Engineering Aspects, 322, 2008, 47-53.

[12] Z. Zhang, Y. Yuan, L. Liang, Y. Cheng, H. Xu, G. Shi and L. Jin, Preparation and photoelectrochemical properties of a hybrid electrode composed of polypyrrole encapsulated in highly ordered titanium dioxide nanotube array. Thin Solid Films, 516, 2008, 8663-8667.

[13] Y. Yang, J. Wen, J. Wei, R. Xiong, J. Shi and C. Pan, Polypyrrole-decorated Ag-TiO_2 nanofibers exhibiting enhanced photocatalytic activity under visible-light illumination. ACS applied materials & interfaces 5, 2013, 6201-6207.

[14] F. Duan, Q. Zhang, D. Shi and M. Chen, Enhanced visible light photocatalytic activity of Bi_2WO_6 via modification with polypyrrole. Applied Surface Science 268, 2013, 129-135.

[15] S.K. Moosvi, K. Majid and T. Ara, Synthesis and characterization of PPY/K$[Fe(CN)_3(OH)(en)]$ nanocomposite: Study of photocatalytic, sorption, electrical, and thermal properties. Journal of Applied Polymer Science 133(23), 2016, DOI: 10.1002/APP.43487.

[16] M. H. Najar and K. Majid, Enhanced photocatalytic activity exhibited by PTh/$[Fe (CN)_3(NO)(bpy)]\cdot 4H_2O$ nanocomposite fibers via a synergistic approach. RSC Advances, 5, 2015, 107209-107221.

[17] W. Naqash, K. Majid, Synthesis, characterisation and study of thermal, electrical and photocatalytic activity of nanocomposite of PANI with $[Co(NH_3)_4(C_{12}H_8N_2)]Cl_3\cdot 5H_2O$ photoadduct. Chemical Physics, 478, 2016, 118-125.

[18] K. Majid, R. Tabassum, A.F. Shah, S. Ahmad, and M.L. Singla, Comparative study of synthesis, characterization and electric properties of polypyrrole and polythiophene composites with tellurium oxide. Journal of Materials Science: Materials in Electronics, 20, 2009, 958-966.

[19] S. K. Moosvi, K. Majid and T. Ara, Studying the electrical, thermal, and photocatalytic activity of nanocomposite of polypyrrole with the photoadduct of $K_3[Fe(CN)_6]$ and diethylenetriamine, Materials Research, 19, 2016, 983-990.

[20] J.A. Khan, M. Qasim, B.R. Singh, S. Singh, M. Shoeb, W. Khan, D. Das and A.H. Naqvi, Synthesis and characterization of structural, optical, thermal and dielectric properties of polyaniline/$CoFe_2O_4$ nanocomposites with special reference to photocatalytic activity. Spectrochimica Acta Part A: Molecular and Biomolecular Spectroscopy, 109, 2013, 313-321.

[21] K. Anandan and V. Rajendran, Influence of dopant concentrations (Mn = 1, 2 and 3 mol%) on the structural, magnetic and optical properties and photocatalytic activities of SnO_2 nanoparticles synthesized via the simple precipitation process. Superlattices and Microstructures, 85, 2015, 185-197.